

Cholinergic Induction of Oscillations in the Hippocampal Slice in the Slow (0.5–2 Hz), Theta (5–12 Hz), and Gamma (35–70 Hz) Bands

Jean-Marc Fellous^{1*} and Terrence J. Sejnowski^{1,2}

¹Computational Neurobiology Laboratory, Howard Hughes Medical Institute, Salk Institute for Biological Studies, La Jolla, California

²Department of Biology, University of California at San Diego, La Jolla, California

ABSTRACT: Carbachol, a muscarinic receptor agonist, produced three distinct spontaneous oscillations in the CA3 region of rat hippocampal slices. Carbachol concentrations in the 4–13 μM range produced regular synchronized CA3 discharges at 0.5–2 Hz (carbachol-delta). Higher concentrations (13–60 μM) produced short episodes of 5–10 Hz (carbachol-theta) oscillations separated by nonsynchronous activity. Concentrations of carbachol ranging from 8–25 μM also produced irregular episodes of high-frequency discharges (carbachol-gamma, 35–70 Hz), in isolation or mixed with carbachol-theta and carbachol-delta. At carbachol concentrations sufficient to induce carbachol-theta, low concentrations of APV reversibly transformed carbachol-theta into carbachol-delta. Higher concentrations of D,L-2-amino-5-phosphonopentanoic acid (APV) reversibly and completely blocked carbachol-theta. A systematic study of the effects of carbachol shows that the frequency of spontaneous oscillations depended nonlinearly on the level of muscarinic activation. Field and intracellular recordings from CA1 and CA3 pyramidal cells and interneurons during carbachol-induced rhythms revealed that the hippocampal circuitry preserved in the slice was capable of spontaneous activity over the range of frequencies observed in vivo and suggests that the presence of these rhythms could be under neuromodulatory control. *Hippocampus* 2000;10:187–197. © 2000 Wiley-Liss, Inc.

KEY WORDS: acetylcholine; rhythms; hippocampus; carbachol; EEG

INTRODUCTION

In the freely moving rat, three types of hippocampal oscillatory activity have been observed that depend on the behavior of the animal (Leung et al., 1982). Low-frequency (0.5–20 Hz) irregular oscillations that predominate during slow-wave sleep are completely absent throughout exploration. Rhythmical components with medium frequencies (5–10 Hz) predominate during exploration and rapid eye movement (REM) or paradoxical sleep, and are absent during slow-wave sleep. Finally, a fast oscillatory component (40–100 Hz) can be observed during REM sleep or exploration. The neuronal mechanisms underlying these oscillations are still largely unknown,

but are likely to involve the complex interplay between intrinsic cellular and synaptic hippocampal properties, and external rhythmical inputs from subcortical areas. Here we focus on the intrinsic hippocampal circuitry and show that rhythms in these three frequency ranges may be observed in an in vitro slice preparation with different concentrations of carbachol present.

The links between hippocampal rhythms in vivo and in vitro have been controversial. The finding that rhythms found in vitro have significant differences with their in vivo counterparts led some researchers to conclude that in vivo preparations are more relevant to epilepsy than to rhythmic phenomena observed in vivo (Traub et al., 1992; Williams and Kauer, 1997). The results reported here emphasize the similarity rather than the differences between in vitro and in vivo preparation. Thus, the rhythmic activity observed in vitro might be supported *in part* by the intrinsic cellular and elementary network properties that are preserved in vitro (Konopacki, 1998). Although hippocampal in vivo rhythms are more complex, the intrinsic mechanisms observed in vitro may serve as a starting point, much as the study of thalamic rhythms benefited by recordings from slices (Steriade et al., 1993b).

Slow Rhythms

In vivo studies have shown that a slow rhythm (<1 Hz) can be found in intracellular recordings in cortical association areas 5 and 7, motor areas 4 and 6, and visual areas 17 and 18 (Steriade et al., 1993e) and in the thalamus (Steriade et al., 1993b) of cats and in the EEG of naturally sleeping cats and humans (Steriade et al., 1993e). This rhythm is thought to be generated by a complex interaction between pyramidal cells and local inhibitory neurons in the cortex and, unlike delta and spindle rhythms, can exist without the thalamus (Steriade et al., 1993d; Timofeev and Steriade, 1996). Because of its ubiquity, this rhythm must be an essential property of the neocortex and the hippocampus.

Grant Sponsor: Howard Hughes Medical Institute.

*Correspondence to: Jean-Marc Fellous, Computational Neurobiology Laboratory, Salk Institute for Biological Studies, 10010 N. Torrey Pines Road, La Jolla, CA 92037. E-mail: fellous@salk.edu
Accepted for publication 23 November 1999

The activation of muscarinic receptors by stimulation of the pedunculopontine tegmental cholinergic nucleus abolishes the slow rhythm in single cells, and shifts the EEG toward higher frequencies (Steriade et al., 1993a). These results suggest that acetylcholine may participate in the regulation of this rhythm, possibly through its effect on calcium-dependent potassium currents: low acetylcholine concentration may promote the slow rhythm, while higher concentrations, by blocking afterhyperpolarizations, may allow fast rhythmic activity to develop.

In the intact hippocampus of urethane-anesthetized rats, oscillatory activity of a frequency as low as 0.5 Hz and large amplitude may be detected (Bland and Colom, 1993). This large irregular activity (LIA) appears in alternation with another oscillatory activity, theta, occurring at higher frequency and which will be discussed below. In vivo experiments show that hippocampal cells may be classified depending on their response to these oscillations: Theta-on cells (putative pyramidal or granule cells) are more active during theta than LIA, and theta-off cells (putative inhibitory interneurons) are more active during LIA than theta. A reduction of acetylcholine levels induces LIA activity, and an increase in acetylcholine induces theta activity. Interestingly, the finding that only theta-on cell activity is correlated with acetylcholine levels suggests that the occurrence of LIA or theta might depend on modulation by septal cholinergic inputs of the balance between excitation and recurrent inhibition in the hippocampal network.

A recent study in hippocampal slices showed that a slow rhythmic activity might be induced by blockade of the Cs-sensitive potassium current (Zhang et al., 1998). It was found in all hippocampal subfields as well as in parietal cortex and originates from a GABAergic interneuronal network, possibly coupled by gap-junctions. Even though in vivo and in vitro slow rhythms may be mediated by different mechanisms, this study clearly shows that slow oscillations are a basic property of the hippocampal network found in slices.

If indeed this slow rhythm is generated by intrinsic properties of the hippocampal tissue, and if, as suggested by in vivo studies, acetylcholine can modulate this rhythm, the question remains as to whether an isolated hippocampal slice can oscillate at this slow frequency under cholinergic modulation.

Theta Rhythm

The theta rhythm has been implicated in several brain functions, including sensory processing, memory, and the control of voluntary movement (Bland, 1986; Bland and Colom, 1993; Vinogradova, 1995). In vivo studies suggest that the hippocampal theta rhythm depends on GABAergic and cholinergic inputs from the septum (Brazhnik and Fox, 1997; Stewart and Fox, 1990) and requires an intact hippocampal CA3 region (Wiig et al., 1994). Cholinergic inputs to the hippocampus are distributed on both pyramidal and interneuronal cells (Frotscher and Leranth, 1985), while GABAergic inputs selectively contact hippocampal interneurons (Freund and Antal, 1988). Complete inactivation of the cholinergic and GABAergic septal inputs results in the blockade of theta activity; infusion of carbachol and picrotoxin, or glutamate and picrotoxin, restored the oscillatory activity, showing that, in

vivo, the hippocampus can be activated and produce theta-like activity in the absence of the septum (Colom et al., 1991; Heynen and Bilkey, 1991; Monmaur et al., 1993). Selective septohippocampal cholinergic lesions sparing GABAergic inputs (Brazhnik et al., 1993; Lee et al., 1994), and in vivo microdialysis studies (Monmaur et al., 1997), have shown that the septal cholinergic input modulates the amplitude but not the frequency of theta. Septal acetylcholine controls the excitability of both pyramidal cells and interneurons, and influences the size of the population involved in the theta rhythm. In in vivo anesthetized preparations, pyramidal cells receive rhythmic GABAergic inputs modulated at theta frequencies that are likely to arise from nearby basket cells (Soltesz and Deschenes, 1993; Ylinen et al., 1995b). These basket cells are themselves paced by GABAergic septal afferents (Stewart and Fox, 1990; Toth et al., 1997). Together, these studies have shown that GABAergic septal inputs may rhythmically hyperpolarize hippocampal basket cells, providing periodic disinhibition of pyramidal cells and perhaps sculpting the hippocampal theta oscillation. Thus, in anesthetized animals, septal cholinergic inputs modulate the power of the theta oscillation, while septal GABAergic inputs determine the temporal pattern. Studies in behaving animals, however, revealed that the rhythmicity of both GABAergic and cholinergic septo-hippocampal inputs were too variable and irregular to account for the observed robustness of the theta rhythm (King et al., 1998). Moreover, recent work in vitro on septo-hippocampal cocultures showed that CA3, but not CA1, exhibited theta-like oscillations driven by septal muscarinic synaptic inputs (Fischer et al., 1999). This suggests that the hippocampus is locally capable of regulating the frequency of theta, independent of septal inputs.

Other studies have shown that theta episodes recorded in the hippocampus can be elicited by stimulation of hypothalamo-septal fibers (Smythe et al., 1991), stimulation of the reticular formation (Kirk and McNaughton, 1993; Vertes, 1982), or by hippocampal infusion of carbachol after posterior hypothalamic inactivation (Oddie et al., 1994).

There is some evidence that hippocampal cells intrinsically resonate at theta frequency, and that when coupled by synaptic transmission in the slice, are capable of synchronized population oscillations. In hippocampal slices, in the absence of synaptic transmission, pyramidal cells present intrinsic subthreshold membrane potential oscillations in the theta range in response to depolarizing currents (Leung and Yim, 1991). These oscillations are the results of the complex interplay between sodium and TEA-sensitive potassium currents. Moreover, when injected with sinusoidal currents of varying frequencies, CA1 pyramidal cells are found to resonate at theta frequency (Leung and Yu, 1998). Partly because of this resonance phenomenon, and because of the properties of interneuron projections to pyramidal cells, single GABAergic cells can effectively pace pyramidal-cell targets at theta frequency (Cobb et al., 1995). Modeling studies of neocortical neurons have explored such phase locking and entrainment issues (Lytton and Sejnowski, 1991).

The hippocampal network is capable of spontaneous activity at theta frequency when activated by muscarinic receptor agonists in slice preparations where septal inputs are absent (Konopacki et al.,

1987; Bland et al., 1988; MacVicar and Tse, 1989). Unlike *in vivo* theta, this rhythm was generated in the CA3 region, and was mediated by non-NMDA excitatory synaptic transmission. It propagated to CA1 and the dentate gyrus, and its propagation to CA1 depended on NMDA synaptic transmission (Williams and Kauer, 1997). However, GABAergic transmission has been shown to synergistically contribute to this rhythm (Heynen and Bilkey, 1991; Konopacki and Golebiewski, 1993), even though it is insufficient to trigger theta oscillations by itself. Different classes of interneurons have been identified on the basis of their firing pattern during carbachol-induced theta (McMahon et al., 1998).

Together, these findings suggest that *in vitro* theta oscillations are the result of the complex interplay between synaptic and intrinsic phenomena that are related to their *in vivo* counterpart. *In vivo* hippocampal theta, therefore, is the result of three phenomena that can be studied independently: external (septum and/or posterior hypothalamic) rhythmic cholinergic and GABAergic inputs, intrinsic network reverberation of CA3 pyramidal and interneuronal populations, and intrinsic single-cell membrane resonance.

Here we show that this rhythm is one of several carbachol-induced rhythms of the hippocampal slice, and we characterize it in relation to two other rhythms.

Fast Rhythms

Synchronous gamma (40–100 Hz) activity has been observed in numerous brain structures (Bressler, 1990; Demiralp et al., 1996; Gray, 1994). *In vivo*, in the hippocampus, this oscillation appears to be controlled by the dentate gyrus and to project to CA3 and CA1, though it is less coherent there (Bragin et al., 1995). However, lesions of the entorhinal cortex shift the site of gamma oscillation generation from the dentate, to the CA3-CA1 system, indicating that, by itself, CA3-CA1 can oscillate at this frequency. Interestingly, the amplitude and frequency between theta and gamma activity were strongly correlated, even when the entorhinal cortex was removed (Bragin et al., 1995).

Recent studies have also shown that hippocampal gamma oscillations can be obtained *in vitro*. Simple repeated stimulation of CA1 afferents, in the absence of any drugs (Whittington et al., 1995), may induce gamma oscillations. Pressure ejection of glutamate, despite blockade of AMPA, NMDA, and GABA_B transmission, may also elicit this oscillation, while GABA_A antagonists or metabotropic glutamate receptor antagonists block it. These results support the hypothesis that, in the slice, gamma oscillations are generated by GABA_A synaptic transmission (Traub et al., 1996; Wang and Buzsaki, 1996), coupled with cellular mechanisms downstream to metabotropic glutamate receptor activation.

Recently, researchers have found that carbachol alone could induce spontaneous epochs of gamma oscillations in the CA3 region of the hippocampal slice (Fellous et al., 1998; Fellous and Sejnowski, 1998; Fisahn et al., 1998). This oscillation is essentially mediated by non-NMDA receptor activation, and its frequency may be altered by modulating the decay time constant of inhibitory post-synaptic potentials (IPSPs) (Fisahn et al., 1998).

MATERIALS AND METHODS

All experiments were carried out in accordance with animal protocols approved by the Salk Institute. Young (20–30 day old) Sprague-Dawley rats were anesthetized using metofane and decapitated, and their brains were quickly removed in cold ACSF. After freehand razor cuts, brains were placed on a vibratome (series 1000), and 400- μ m transversal hippocampal slices were obtained. Slices were held in ACSF in mM: NaCl, 124; NaH₂CO₃, 26; D-glucose, 10; KCl, 5; CaCl₂, 2; MgSO₄, 2; and NaH₂PO₄, 1.2, saturated with 95% O₂/5% CO₂, at room temperature. Prior to transfer to the submerged recording chamber, some slices underwent razor cuts to isolate CA3. Intact or “mini” slices were then placed in the recording chamber, at 31–32°C, and perfused at constant flow (2–3 ml/min). Unless otherwise noted, results are presented for whole-slice experiments.

Field recordings were obtained with glass microelectrodes (ACSF filled, 300–400 K Ω), pulled using a Flaming/Brown micropipette puller (P97, Sutter Instruments) and placed in the cell body layer in CA1 or CA3. Whole-cell patch-clamp recordings were achieved using glass electrodes containing (4–10 M Ω) mM: KmeSO₄, 140; HEPES, 10; NaCl, 4; EGTA, 0.1; Mg-ATP, 4; Mg-GTP, 0.3; and phosphocreatine, 14. Patch-clamp was performed under difference interference contrast (D.I.C.) visual control. In most experiments, Lucifer Yellow (0.4%, RBI) was added to the internal solution. At the end of each experiment, high-intensity mercury blue light was shined on the cell recorded. Fluorescence was recorded on videotape. Cells were characterized as pyramidal or interneurons on the basis of their morphology and physiological responses to square pulses (spike half width, size of fast afterhyperpolarization, and presence of spike frequency adaptation). Pyramidal cells had a large number of spines, while interneurons did not. Pyramidal-cell morphologies were similar to those published in the literature. In a few instances (~2 CA1, ~3 CA3), pyramidal cells were found to have a primary stem cut and were rejected. All drugs were obtained from RBI or Sigma (St. Louis, MO), freshly prepared in ACSF, and bath-applied. Data were acquired with Labview 5.0 and a PCI-16-E1 data acquisition board (National Instrument, Baltimore, MD), and analyzed with Matlab (The Mathworks) and Excel (Microsoft, Redmond, WA).

RESULTS

Of 150 slices tested, about 100 showed a predictable pattern of increased spontaneous activity followed by stable synchronized discharges when carbachol was continuously applied. The other 50 slices did not show increased single-cell spontaneous activity when carbachol was applied, or showed such increased activity, but failed to synchronize in population bursts. The results presented here are based on the 88 slices that had the best electrical recordings (least noise). In all, 16 interneurons in CA3, 8 interneurons in CA1, and 9 pyramidal cells in CA3 were recorded intracellularly.

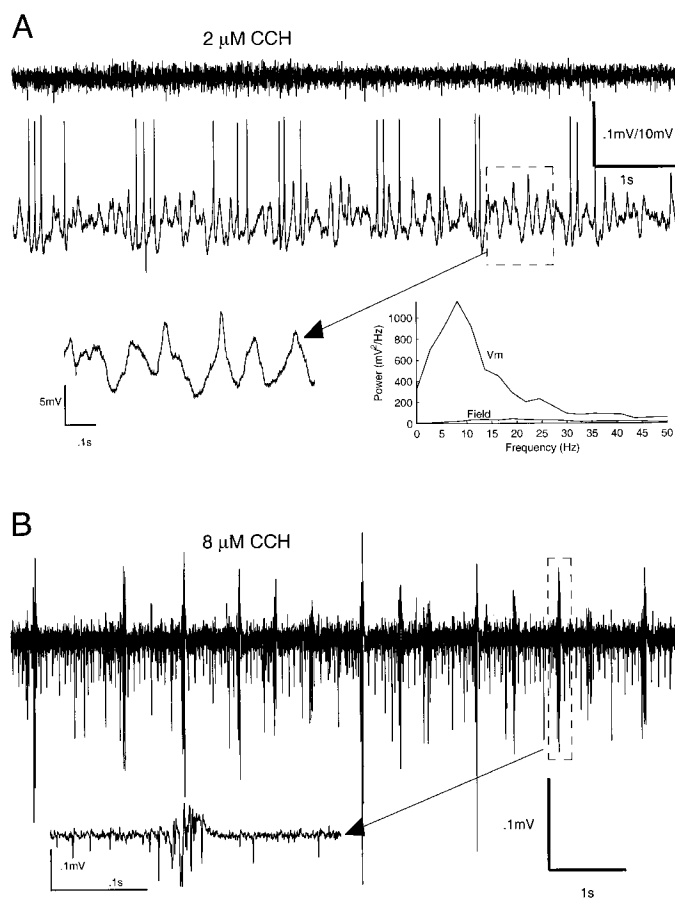


FIGURE 1. Effects of low concentrations of carbachol in CA3. **A:** Simultaneous field recording (top) and whole-cell recording from a CA3 pyramidal cell (bottom). Low concentration ($2 \mu\text{M}$) of carbachol produced membrane oscillations and spiking. Inset, lower left: Expanded view of oscillatory activity (dashed box). Inset, lower right: Power spectrum of the membrane potential (upper trace, action potentials clipped, peak at 9.8 Hz) and the field recording (lower trace, no peaks). **B:** Slow rhythmic activity in $8 \mu\text{M}$ carbachol measured by field recording in the cell body layer of CA3. Inset: Single spike activity before and after the population discharge (expanded from dashed box). In all figures, voltage scales are given for field and whole-cell recordings, respectively.

Bath application of carbachol at all the concentrations used in this study ($2\text{--}60 \mu\text{M}$) depolarized all cells that were recorded. Results are given as mean \pm standard deviation.

Subthreshold Oscillations

Low concentrations of carbachol ($2\text{--}4 \mu\text{M}$) induced irregularly spaced bouts of spontaneous membrane potential oscillations in the $5\text{--}10$ Hz range. These oscillatory episodes lasted a few seconds and were sometimes accompanied by riding spikes ($n = 14/15$, Fig. 1A). These oscillations were present in CA3 pyramidal cells ($n = 5/6$) and interneurons in CA1 ($n = 3$) and CA3 ($n = 6$). Blocking synaptic transmission (CNQX $10 \mu\text{M}$, APV $50 \mu\text{M}$, bicuculline $20 \mu\text{M}$) reduced the amplitude, but not the occurrences of these oscillations ($n = 3$ CA3 pyramidal cells, $n = 2$ CA1 interneurons).

Higher concentrations of carbachol ($4\text{--}60 \mu\text{M}$) produced three distinct types of spontaneous synchronous discharges that are detailed below.

Carbachol-Delta

Low concentrations of carbachol ($4\text{--}13 \mu\text{M}$) produced a regular pattern of synchronous discharges (Fig. 1B) that we call carbachol-delta. The frequency was in the delta range of $0.5\text{--}2$ Hz (0.85 ± 0.33 Hz, $n = 16$, $4\text{--}13 \mu\text{M}$ carbachol) and did not significantly depend on the concentration of carbachol applied. The duration of each discharge was less than 100 ms (Fig. 1B, inset). This rhythmic pattern originated in CA3, as assessed by isolating CA3 from CA1 and the dentate, and was blocked by atropine sulfate ($2 \mu\text{M}$, $n = 2$) or CNQX ($10 \mu\text{M}$, $n = 3$, data not shown). Intracellular recordings showed that spontaneously active CA1 interneurons were phasically recruited during carbachol-delta ($n = 4/5$, Fig. 2A, left), indicating that the synaptic drive from CA3 to CA1 was sufficient to pace the CA1 interneuronal network.

Carbachol-Theta

Higher concentrations of carbachol ($13\text{--}60 \mu\text{M}$) produced a markedly different pattern of discharges (Fig. 2A (right), B) that consisted of short episodes (~ 10 s) of synchronous population discharges at a regular frequency ($5\text{--}10$ Hz, mean 8.2 Hz, $n = 41$, $25 \mu\text{M}$ carbachol). The start and end of each episode were typically abrupt, with a slight increase and decrease (~ 1 Hz) of frequency. Two episodes were separated by about $20\text{--}30$ s of single-cell activity measured with field electrodes, but with no synchronous discharges. Using the minislice preparation, we confirmed that these discharges originated in CA3 and propagated to CA1 (see also Williams and Kauer, 1997). Cuts of isolated CA1 and dentate gyrus specifically excluded the CA3 circuitry. This oscillation was found in isolated CA3, but not in isolated CA1, and dual field recordings in CA3 and CA1 revealed a positive latency (about $10\text{--}15$ ms) in CA1 ($n = 3$, data not shown). This oscillation was never found in isolated dentate gyrus ($n = 3$, data not shown).

CNQX ($10 \mu\text{M}$) added to $25 \mu\text{M}$ carbachol was effective in reversibly blocking this oscillation in CA3 ($n = 2/2$, data not shown). APV ($50 \mu\text{M}$), when coapplied with high concentrations of carbachol ($25\text{--}50 \mu\text{M}$), was effective in attenuating the transmission of this oscillation from CA3 to CA1 ($n = 5/8$, data not shown; see also Williams and Kauer, 1997), although no effects were noticeable in $3/8$ cases. Atropine ($2 \mu\text{M}$) was effective in preventing carbachol-induced oscillations ($n = 3$ at $25 \mu\text{M}$ carbachol, $n = 2$ at $50 \mu\text{M}$ carbachol; see also MacVicar and Tse, 1989). Bicuculline ($20 \mu\text{M}$) had no consistent effects on the ongoing oscillations ($n = 5$; but see Konopacki and Golebiewski, 1993), indicating that neurotransmission through GABA_A receptors was not primarily involved. These results are compatible with others showing that this oscillation is mainly mediated by non-NMDA excitatory neurotransmission (Traub et al., 1992; Williams and Kauer, 1997).

Dual-field and single-cell recordings in CA3 showed that pyramidal cells were depolarized during population discharges ($25 \mu\text{M}$

carbachol) and fired at most once per cycle ($n = 6$), in synchrony with field events (Fig. 3A). Depolarization or hyperpolarization by constant current injection affected the probability of firing, but, unlike *in vivo* recordings (Soltesz and Deschenes, 1993), did not alter the phase relationship between single-cell and field events. Firing occurred typically once every 3–5 cycles, started shortly (100 ms) before the field events were detected, and continued a few seconds afterwards, albeit at a lower frequency (2–3 Hz slower than the preceding carbachol-theta episode).

As shown in Figure 3B, CA3 interneurons became tonically active with 25 μM carbachol in the bath (McMahon et al., 1998). The frequency of firing was within the theta range (7.2 ± 1.3 Hz, $n = 10$, 25 μM carbachol, Fig. 3B) and was present throughout each experiment. Six out of 10 interneurons were tonically inhibited by an ongoing carbachol-theta episode (Fig. 3B), and their firing frequency decreased (mixed class II/III in McMahon et al.,

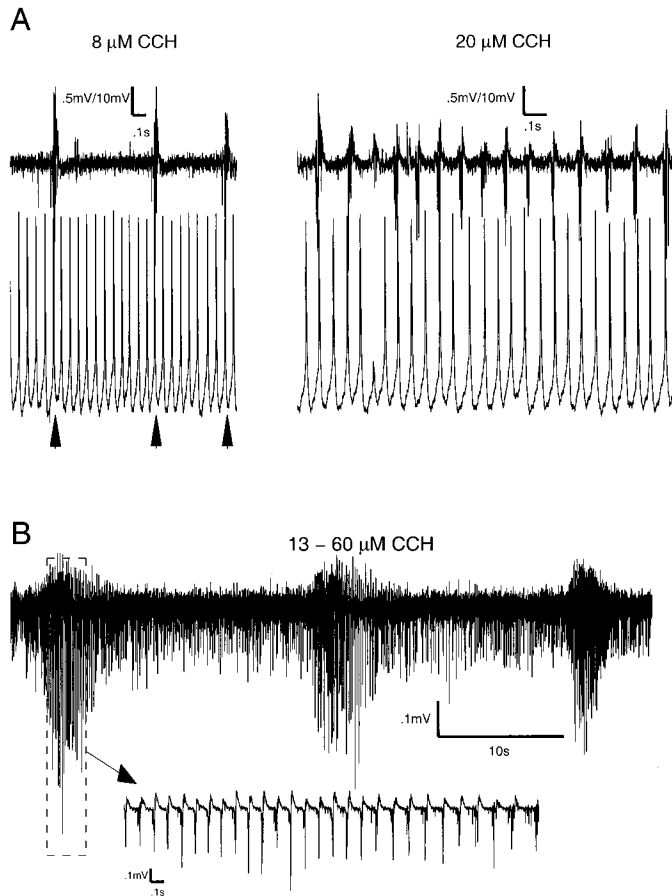


FIGURE 2. Carbachol-theta in CA1 and CA3. **A:** CA1 interneuron membrane potential (lower trace) and field recording (upper trace) in CA3. Interneurons were recruited by the CA3 carbachol-delta discharges (left, 8 μM carbachol), but not during carbachol-theta (right, 20 μM carbachol). Note the small depolarizations (arrowheads) induced by the CA3 population events. **B:** Field recordings of three consecutive CCh-theta episodes. Higher concentration of carbachol (13–60 μM) produced a stereotypical pattern of carbachol-theta oscillations (here obtained with 20 μM). The lower trace is an expanded view of the dashed box showing the synchronous population discharges (here about 10 Hz).

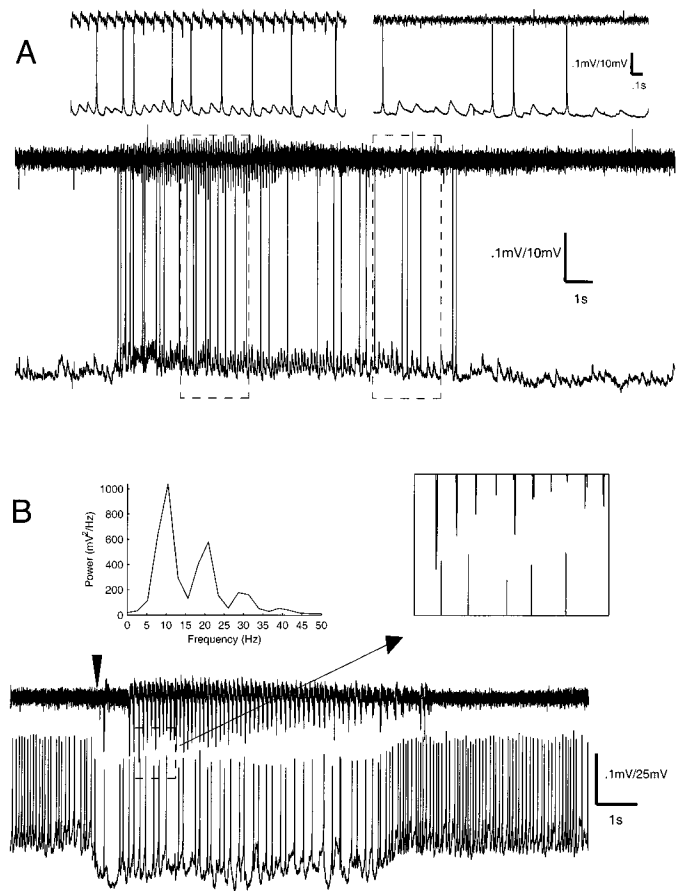


FIGURE 3. Carbachol-theta in CA3 pyramidal cells and interneurons. **A:** Pyramidal cells were depolarized during the population discharge (field recording, upper trace; whole-cell recording, lower trace). Left inset (above): Expanded section (from left dashed box) showing that the firing of the pyramidal cell was synchronous with field events during CCh-theta, but that the cell did not fire on each cycle. Right inset (above): Expanded section (from right dashed box) shows that the pyramidal cell received few additional membrane oscillations at lower frequencies, once the field discharges were terminated. **B:** This CA3 interneuron became tonically active as soon as 25 μM of carbachol were added to the perfusate before recording. A theta episode begins spontaneously (arrowhead) and the interneuron is hyperpolarized. Left inset (above): Power spectrum indicates a clear peak within the theta band. During the carbachol-theta discharges, the interneuron decreased its firing frequency and stayed desynchronized with field activity (right inset; expanded from dashed box).

1998). Two out of 10 interneurons were not affected by the CA3 population bursts (class III in McMahon et al., 1998). Two interneurons were synchronized with field events (class I in McMahon et al., 1998).

Carbachol-delta was also present during the washout of high (>20 μM) concentrations of carbachol, but was never present simultaneously with carbachol-theta. Continuously decreasing the concentration of carbachol yielded an abrupt and stable transition between carbachol-theta and carbachol-delta (Fig. 7). Interestingly, most CA1 interneurons fired synchronously with carbachol-delta, but not carbachol-theta ($n = 4/5$, Fig. 2A), while previous work showed that the amplitudes of carbachol-theta bursts were

significantly smaller than the carbachol-delta discharges, measured in the same slice (Fellous et al., 1998). Together, these results indicated that carbachol-delta was either more synchronous, or involved more neurons than carbachol-theta. Finally, at concentrations of carbachol just sufficient to transform carbachol-delta into a stable carbachol-theta (around 20 μM , depending on the slice), low concentrations of APV (10 μM) reversibly transformed carbachol-theta into carbachol-delta ($n = 3$, Fig. 4A–C). In this condition, higher concentrations of APV (>50 μM) reversibly blocked carbachol-theta ($n = 3$, Fig. 4D). At higher carbachol concentrations ($\geq 50 \mu\text{M}$), APV (10–50 μM) was ineffective in blocking carbachol-theta ($n = 4$, data not shown).

Carbachol-Gamma

Concentrations of carbachol in the 8–25 μM range often produced faster population discharges in the gamma band in both

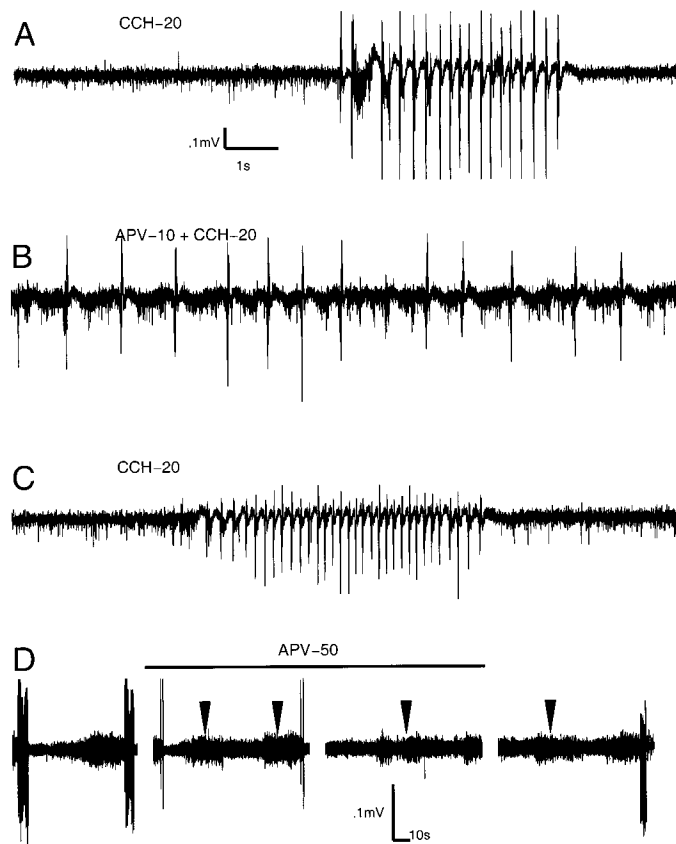


FIGURE 4. Effects of high and low concentrations of APV on carbachol-induced oscillations. Field recording in CA1 in “threshold” carbachol-theta carbachol concentrations (20 μM). A–C: Traces from the same slice. A: Carbachol-theta. B: After 10 μM APV were added to the carbachol solution, the carbachol-theta rhythm transformed into carbachol-delta. C: After APV was washed out, the carbachol-theta rhythm returned. D: On a different slice, 50 μM APV blocked carbachol-theta; 20 μM carbachol were present before the start of the recording and during the whole experiment. Note that the increase of single-cell activity before carbachol-theta bursts persisted during APV (arrowheads), even though no synchronous discharges were produced. The four successive recordings were separated by 3–4 min.

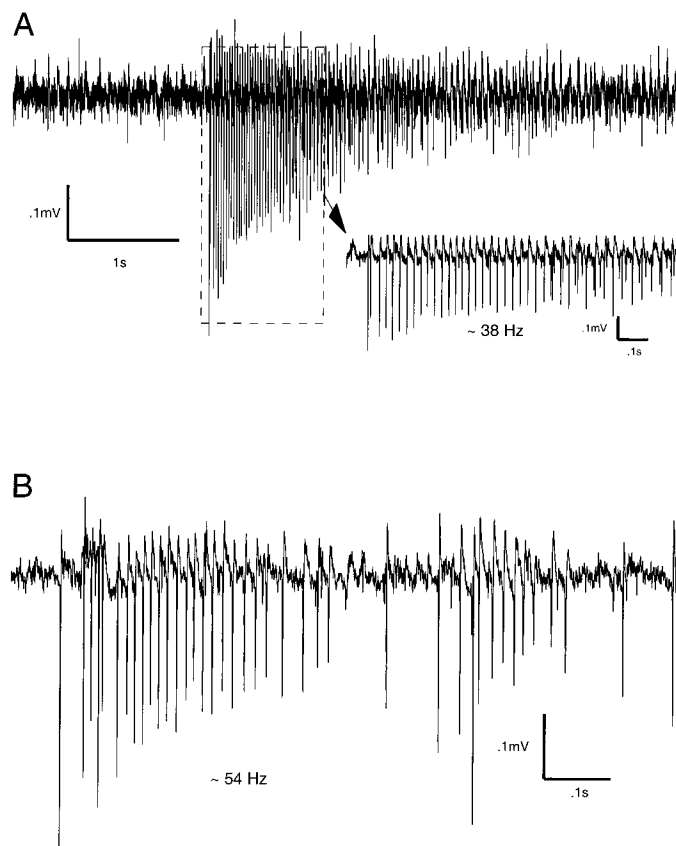


FIGURE 5. Carbachol-gamma in 8 μM carbachol, measured with field recordings. A: Spontaneous episode of carbachol-gamma in CA1. Frequency is about 38 Hz. B: Spontaneous episode of carbachol-gamma in CA3. Frequency is about 54 Hz.

CA1 and CA3 (Fig. 5A,B). These oscillations occurred spontaneously in the absence of other frequencies, or mixed with carbachol-delta or carbachol-theta (Fig. 6A,B). When measured during their isolated occurrences, these oscillations were somewhat faster in CA3 ($57.6 \pm 3.5 \text{ Hz}$, $n = 3$) than in CA1 ($42 \pm 4 \text{ Hz}$, $n = 3$) and lasted at least 500 ms ($726 \pm 207 \text{ ms}$, $n = 6$). No other isolated oscillations of such duration were observed. This oscillation was present in CA3 minislices, but was never observed in CA1 minislices. It was never observed in the presence of bicuculline ($n = 3$, 10 μM). Due to the randomness of these fast discharges, a precise quantitative analysis was not possible. However, others have reported fast oscillations in a similar slice preparation (Fisahn et al., 1998). In that study, the oscillation was persistent and carbachol-theta was intermittent, whereas our observations showed robust theta oscillations and irregular gamma episodes. This discrepancy might be due to slight differences in the way the hippocampal slices were cut (O. Paulsen, personal communication).

Figure 7 presents a summary of the results of this study. Low concentrations of carbachol (4–13 μM) induced persistent carbachol-delta activity (below the dashed line), while higher concentrations (13–60 μM) induced carbachol-theta patterns of oscillations. Carbachol-gamma (mixed with carbachol-theta or carbachol-delta or in isolation) was seen only at carbachol concentrations ranging between 8–25 μM . Carbachol-gamma appeared

to be independent from the other two rhythms, possibly involving a separate mechanism.

DISCUSSION

The hippocampal rhythms observed *in vivo* are the result of a complex interplay between cellular and synaptic properties within the hippocampus, and extrahippocampal tonic as well as oscillatory inputs (Bland, 1986; Dutar et al., 1995; Stewart and Fox, 1990; Vinogradova, 1995). For stable rhythms to occur, the hippocampal circuitry should have the potential to oscillate at those specific frequencies. We have provided evidence that the hippocampal slice can indeed generate oscillations at three different frequency bands that have also been observed *in vivo*. Moreover, the levels of activation of muscarinic receptors alone can determine which pattern of oscillation is most likely to occur (Fig. 7).

Delta Frequency

Several lines of experimental and clinical evidence point toward the involvement of acetylcholine in the modulation of slow (delta-

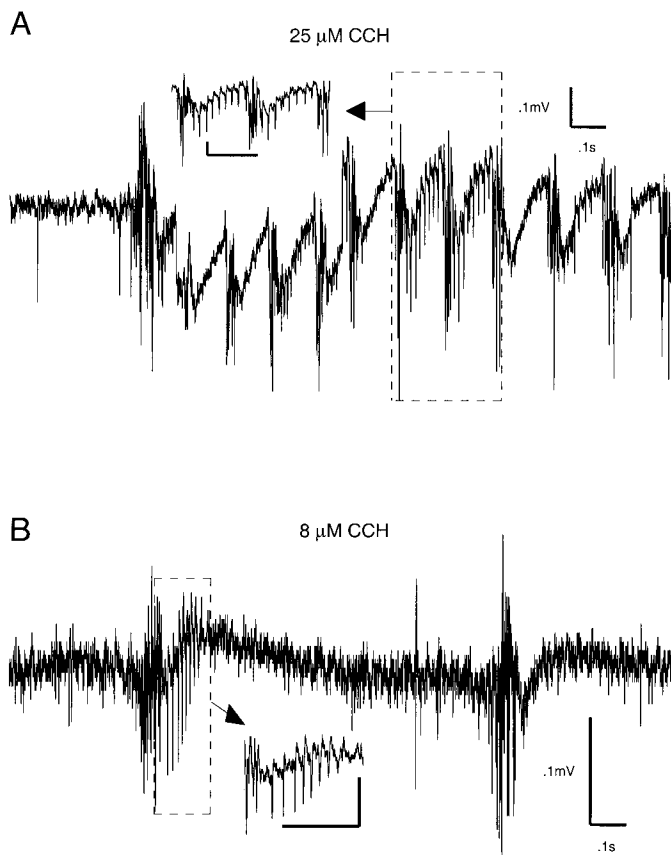


FIGURE 6. Mixed rhythms measured in CA1 with field recordings. **A:** Carbachol-gamma mixed with carbachol-theta, 25 μM carbachol. **B:** Carbachol-gamma mixed with carbachol-delta, 8 μM carbachol. Adapted from Fellous et al. (1998). Insets, **A** and **B:** Enlargements of dashed boxes; scale is 0.1 mV/0.1 s for both.

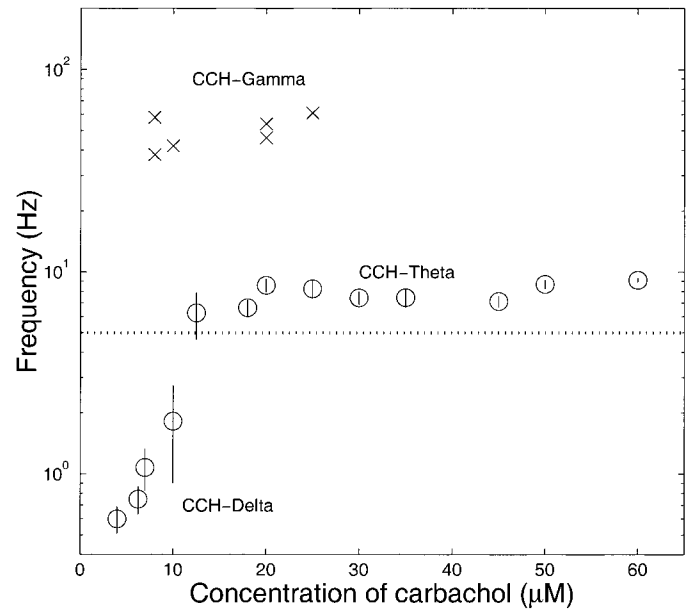


FIGURE 7. Dose/frequency curve. At low concentrations of carbachol (4–13 μM), CA3 neurons discharge regularly and synchronously at low frequencies (0.5–2 Hz, Figs. 1B, 4B). At higher concentrations (13–60 μM) CA3 follows the carbachol-theta pattern (5–10 Hz, Fig. 2B). At intermediate concentrations (8–25 μM) spontaneous transient field discharges at carbachol-gamma (45–61 Hz, Figs. 5, 6) frequencies often occur. Points marked O are the average of at least three slices. Points marked X are individual measurements. The dashed line is placed at 5 Hz and separates the delta and theta temporal patterns (regular patterns as in Figs. 1B, 4B are below the line; waxing and waning patterns as in Fig. 2B are above the line). Vertical bars on open symbols are error bars (± SD). Carbachol-delta frequency was measured on the basis of at least 5 s of consecutive data, carbachol-theta frequency was measured as the average of at least three consecutive oscillating episodes, and carbachol-gamma was measured on the basis of individual occurrences.

like) EEG activity in the cortex (Steriade et al., 1993e), thalamus (Riekkinen et al., 1991), and nucleus accumbens (Leung and Yim, 1993). Reduction of cholinergic activity induced a slowing of the EEG that is qualitatively compatible with the results reported here. The slow spontaneous oscillations observed *in vitro* under low carbachol concentrations may therefore support *in vivo* brain activity such as delta rhythms, large irregular activity, the initiation of sharp waves, and slow rhythmic oscillations observed during deep sleep.

In our experiments, carbachol-delta oscillations were never present with carbachol-theta, indicating that these rhythms are two distinct modes of oscillations in the slice, which is compatible with other *in vitro* (Boguszewicz et al., 1996) and *in vivo* (Bland and Colom, 1993) observations. The dependence of these two rhythms on carbachol concentration is also consistent with *in vivo* data showing that the simultaneous occurrence of delta and theta oscillations was rare during human behavior (Meador et al., 1991), and that the increase of endogenous acetylcholine levels with an anti-cholinesterase decreased delta and increased theta in awake rabbits (Brazhnik et al., 1993). In Alzheimer’s disease, where cholinergic neurons in the nucleus basalis degenerate, EEG power in the theta

range decreased while power in the delta range increased (Riekkinen et al., 1991). Finally, selective destruction of septal cholinergic inputs reduced the power of (but did not abolish) hippocampal theta activity. In this condition, peripheral injection of physostigmine, an anticholinesterase, failed to induce theta, but successfully induced slow oscillations (Lee et al., 1994). This result is compatible with the results presented here to the extent that physostigmine may have contributed to the restoration of low levels of hippocampal acetylcholine, mimicking the carbachol-delta rhythm we observed in low concentrations of carbachol, *in vitro*. The mechanisms by which different levels of cholinergic modulation induce such different patterns of oscillations are unclear. However, an earlier modeling study suggested that the selective increase of a calcium-dependent potassium conductance could slow down a carbachol-theta oscillation to frequency ranges similar to carbachol-delta (Traub et al., 1992), partly mimicking the effect of lowering the concentration of carbachol (Fig. 7). Unfortunately, this particular phenomenon was not thoroughly studied, and other effects of carbachol on M-currents and synaptic transmissions were not included in these simulations, possibly explaining why the transition from theta to delta was smooth, while it is sharp according to our experimental results.

Sharp waves *in vivo* originate as synchronized CA3 bursts, and appear when theta and acetylcholine levels are depressed (Bland et al., 1996; Ylinen et al., 1995a), consistent with the presence of slow synchronized activity in the slice at low concentrations of carbachol. Our findings suggest that the initiation of sharp waves, e.g., carbachol-delta, is dependent on low levels of acetylcholine. *In vivo*, this discharge is accompanied by 200-Hz ripples (the LIA/sharp wave complex), while *in vitro* they are often followed by carbachol-gamma (Fig. 6B). Moreover, *in vivo* studies have shown that sharp waves, gamma, and theta have very similar depth profiles (Bragin et al., 1995; Ylinen et al., 1995a). Together, these results suggest that, although the mechanisms underlying theta and LIA/sharp wave oscillations *in vivo* may rely on independent inputs to CA1 (Bland et al., 1996; Leung et al., 1982), they also depend on the cholinergic modulation of the hippocampus: high and low levels of acetylcholine promoting theta and LIA/sharp wave oscillations, respectively.

Finally, it is interesting to note that slow, spontaneous carbachol-dependent discharges can be observed in the entorhinal cortex *in vitro* (Dickson and Alonso, 1997). However, these discharges have a markedly different temporal structure than the carbachol-delta rhythm we described here, including a much longer duration (up to several seconds, vs. less than 0.1 s for carbachol-delta; Fig. 1B, inset) and recurrence at a slower pace (0.01 Hz, vs. 0.5–2 Hz for carbachol-delta). Taken together, these results suggest that the mechanisms underlying entorhinal cortex epileptiform discharges and carbachol-delta are distinct.

Theta Frequency

Simultaneous field and intracellular recordings from CA3 pyramidal cells during carbachol-theta (MacVicar and Tse, 1989) revealed oscillations that were synchronous among pairs of CA3 pyramidal cells, although the latter did not necessarily fire on each

cycle (Fig. 3A). Theta bursts were accompanied by slow glial depolarizations (accumulation of K^+), and single cells were synchronous with field potentials. This oscillation was blocked by bath application of TTX or $CdCl_2$, pointing toward a network phenomenon. GABA_A, GABA_B, and NMDA blockers were ineffective in blocking these rhythms in CA3, but kynurenic acid blocked it. Increases in extracellular Ca^{2+} were also effective in blocking carbachol-theta. Together, these results indicate that carbachol-theta is generated by non-NMDA excitatory synaptic activity among CA3 pyramidal cells.

Interestingly, preincubation of slices in 100 μM APV markedly reduced the propensity for the oscillation to propagate from CA3 to CA1 (Williams and Kauer, 1997). This result indicates therefore that while NMDA transmission is not required for the CA3 genesis of carbachol-theta (induced at 50 μM carbachol), it might be important for its transmission to CA1. Here we have shown that when the slice is bathed in carbachol concentrations *just sufficient* to obtain a stable carbachol-theta (about 20 μM , depending on the slice), both NMDA and non-NMDA receptors were involved. Low concentrations of APV (10 μM) were capable of reversibly returning carbachol-theta into carbachol-delta (Fig. 4A–C), consistent with *in vivo* data showing that intraventricular infusion of APV decreases theta activity and increases large irregular delta-like waves measured in CA1 during immobility (Leung and Desborough, 1988). Such low concentrations of APV have been shown *in vitro* to be effective in blocking NMDA receptors on interneurons, while keeping most of the pyramidal cells receptors active (Grunze et al., 1996). Higher concentrations of APV (>50 μM) blocked 20 μM carbachol-theta, while at higher carbachol concentrations (50 μM), 50 μM APV was ineffective in blocking the oscillation (MacVicar and Tse, 1989; Williams and Kauer, 1997). Our results therefore suggest that, at concentrations of carbachol just sufficient to induce carbachol-theta, selective blockade of NMDA receptors on interneurons may change the dynamics of the CA3 network and modulate the switch between carbachol-delta and carbachol-theta rhythms. Global blockade of NMDA receptors in the whole slice resulted in the complete block of the oscillation (Fig. 4D).

The behavior of interneurons during carbachol-theta has also been examined (McMahon et al., 1998). Three classes of interneurons have been distinguished in 50 μM carbachol. Class I interneurons were depolarized by the carbachol-theta episodes, and were silent otherwise and fired synchronously with field events. Class II interneurons were hyperpolarized during the carbachol-theta bursts and did not fire either before or during the episode. Class III interneurons were spontaneously active, and did not correlate with field recordings. In our study, at 25 μM carbachol, both class I and III interneurons were found (data not shown), as well as mixed class II/III interneurons which were tonically active before carbachol-theta episodes, but hyperpolarized in an asynchronous fashion during the CA3 population discharges (Fig. 3B). This discrepancy might be due to the different concentrations of carbachol used. At the 25- μM carbachol concentration that we used, more inhibitory transmission might be preserved, which may result in a more powerful inhibition of Class III cells.

In contrast to the results presented by others (Williams and Kauer, 1997), CA3 pyramidal cells did not burst at each cycle of

the oscillation. This difference can be partly explained by the lower concentration of carbachol used here (25 vs. 50 μM) and the use of a higher extracellular concentration of KCl (5 vs. 2.5 mM). Lower concentrations of carbachol yielded a lower overall depolarization of all cells, and higher extracellular KCl yielded longer, but smaller amplitude field theta oscillations. Taken together, these differences synergistically contributed to a lower level of depolarization of CA3 pyramidal cells before and during the carbachol-theta burst, hence eliciting single spiking rather than bursting behavior. A separate line of evidence on cocultured septo-hippocampal slices also showed that CA3 cells could undergo synaptic muscarinic oscillation in the theta range without spiking at each cycle (Fischer et al., 1999).

In a previous study, carbachol (25 μM) increased IPSP frequencies of CA1 interneurons from ~ 1 Hz to 6–8 Hz, even in the absence of excitatory transmission, while IPSP amplitudes increased (Pitler and Alger, 1992). This result is compatible with our finding that most CA1 (and CA3) interneurons fired spontaneously in the theta range as soon as carbachol was introduced into the bath. Moreover, our observation that during carbachol-theta, most interneurons were spontaneously active but desynchronized from field events (Fig. 2A) is compatible with the prediction that while carbachol directly excites GABAergic interneurons, it also depresses GABAergic release at inhibitory terminals on pyramidal cells (Behrends and ten Bruggencate, 1993; Patil and Hasselmo, 1999), hence preventing the coupling between interneurons and pyramidal cells. Finally, recent experiments suggest that pyramidal cells are capable of “resonating” at theta frequencies when depolarized by constant current injection or when driven by sine waves of positive mean and frequencies within the theta range (Leung and Yim, 1991; Leung and Yu, 1998). This phenomenon may explain the cellular basis of CA3 carbachol-theta since carbachol, by blocking several potassium currents (I_{AHP} , I_{M} , I_{K} , and $I_{\text{K}}[\text{Ca}]$) (Madison et al., 1987; McCormick, 1989), depolarizes all cells. Because of the resonance of CA cells, firing will preferentially occur at theta frequencies, and through recurrent excitatory transmission will generate synchronized episodes of carbachol-theta, detectable with field recordings. This resonance phenomenon may also be the basis for the theta-range subthreshold oscillation we observed with low (2–4 μM) concentrations of carbachol (Fig. 1A). These observations are compatible with recent theoretical studies showing that comprehensive modeling of the effects of high concentrations of carbachol on intrinsic and synaptic properties may yield spontaneous synchronous network discharges in the theta range, mimicking the results observed here (Liljenstrom and Hasselmo, 1995). Interestingly, that work also showed that higher-frequency oscillations in the gamma range might also appear through the synergistic effects of carbachol modulation and extrinsic stimulation of a population of cells.

Gamma Frequency

In vivo theta activity is sometimes accompanied with high-frequency gamma oscillations (Penttonen et al., 1998), presumably originating in the dentate gyrus (Bragin et al., 1995). Lesion of the entorhinal cortex, however, shifted the locus of generation of this

rhythm to CA3, and slowed its frequency significantly. Current source density revealed that sources and sinks were identical to those obtained during sharp waves (Bragin et al., 1995; Soltesz and Deschenes, 1993; Traub et al., 1996), indicating, as we have suggested, that these two rhythms may involve a similar spatial organization of hippocampal activity. However, theta and gamma activity are correlated in vivo, while in our experiment carbachol-theta and carbachol-gamma were not, suggesting that, in vivo, these two rhythms may share common synchronizing inputs, possibly of septal origin.

In vivo data suggest that the hippocampal gamma rhythm is mediated by interneurons, and its timing and spatial organization have been modeled (Traub et al., 1996; Wang and Buzsaki, 1996; Zhang et al., 2000). However, CA1 pyramidal cells in vivo resonate at gamma frequency when injected with depolarizing current pulses immediately following commissural stimulation (Penttonen et al., 1998). Commissural stimulation has been hypothesized to prevent dendritic calcium spikes in CA1 cells, thereby limiting the calcium-dependent potassium current responsible for spike-frequency adaptation (I_{AHP}). This hypothesis is compatible with in vitro results presented here, in that carbachol reduced I_{AHP} (Madison et al., 1987) and induced depolarization, hence favoring the occurrence of resonating gamma oscillations in pyramidal cells.

Because of the random occurrence of the carbachol-gamma episodes, it was not possible to study here the respective involvement of CA1 and CA3 cells. However, other recent in vitro experiments point to the involvement of the GABAergic interneuronal network in the mediation of this rhythm. Stimulation of CA1 afferents, in conditions where metabotropic glutamate receptors are activated, produced short sequences of gamma subthreshold oscillations that were blocked by bicuculline (Colling et al., 1998; Whittington et al., 1995). Carbachol was also effective in triggering spontaneous gamma oscillations in the hippocampal slice detectable by field recordings (Fellous et al., 1998; Fellous and Sejnowski, 1998) and intracellular recordings (Fisahn et al., 1998). This oscillation originates in CA3 but can be found in CA1 (Figs. 5A, 6), and depends on non-NMDA and GABA_A synaptic transmission (Fisahn et al., 1998). Altogether, these results suggest that carbachol-gamma is mediated by GABAergic transmission among interneurons, and is generated independently from carbachol-theta or carbachol-delta.

In vivo, only a small number of CA3 cells are active carriers of information during theta and gamma oscillations, and these cells are therefore very difficult to study experimentally. However, their role in information processing is essential. Here we showed, in vitro, that it is possible to involve a large number of these cells, during several oscillatory behaviors. Because the oscillations presented here use part of the machinery responsible for their occurrence in vivo, it is hoped that such an in vitro preparation will help to experimentally elucidate the nature of the involvement of CA3 in these rhythms.

In conclusion, we have found that the concentration of carbachol strongly affected the frequencies and time course of spontaneous oscillations in hippocampal slices. There appear to be two incompatible network states, a slow-frequency rhythm that occurs at low carbachol concentrations, and a high-frequency theta-like state at higher concentrations. Intermediate levels of carbachol

induced gamma-like oscillations that were generated by mechanisms different from those responsible for lower frequency rhythms. During slow-wave sleep, medial septal activity (and hence hippocampal cholinergic level) is low, and EEG patterns show slow irregular activity in the delta range. During REM sleep and exploration, septal activity (and hippocampal cholinergic level) is high, and the EEG shows theta rhythmic activity (Dutar et al., 1995; Riekkinen et al., 1991). This suggests that several of the EEG patterns observed *in vitro* are reflected in the dynamics of the cholinergic modulation of the CA3 network *in vitro*, and that this preparation might prove useful for the study of the neural basis of the transitions from one EEG state to another.

Acknowledgments

We thank György Buzsáki for his very insightful comments on the original manuscript and Paul Tiesinga and Gabriele Scheler for many helpful discussions.

REFERENCES

- Behrends JC, ten Bruggencate G. 1993. Cholinergic modulation of synaptic inhibition in the guinea pig hippocampus *in vitro*: excitation of GABAergic interneurons and inhibition of GABA-release. *J Neurophysiol* 69:626–629.
- Bland BH. 1986. The physiology and pharmacology of hippocampal formation theta rhythms. *Prog Neurobiol* 26:1–54.
- Bland, BH, Colom LV. 1993. Extrinsic and intrinsic properties underlying oscillation and synchrony in limbic cortex. *Prog Neurobiol* 41:157–208.
- Bland BH, Colom LV, Konopacki J, Roth SH. 1988. Intracellular records of carbachol-induced theta rhythm in hippocampal slices. *Brain Res* 447:364–368.
- Bland BH, Trepel C, Oddie SD, Kirk IJ. 1996. Intraseptal microinfusion of muscimol: effects on hippocampal formation theta field activity and phasic theta-ON cell discharges. *Exp Neurol* 138:286–297.
- Boguszewicz J, Skrajny B, Kohli J, Roth SH. 1996. Evidence that GABA, serotonin, and norepinephrine are involved in the modulation of *in vitro* rhythmic activity in rat hippocampal slices. *Can J Physiol Pharmacol* 74:1322–1326.
- Bragin A, Jando G, Nadasdy Z, Hetke J, Wise K, Buzsaki G. 1995. Gamma (40–100 Hz) oscillation in the hippocampus of the behaving rat. *J Neurosci* 15:47–60.
- Brazhnik ES, Fox SE. 1997. Intracellular recordings from medial septal neurons during hippocampal theta rhythm. *Exp Brain Res* 114:442–453.
- Brazhnik ES, Vinogradova OS, Stafekhina VS, Kitchigina VF. 1993. Acetylcholine, theta-rhythm and activity of hippocampal neurons in the rabbit—I. Spontaneous activity. *Neuroscience* 53:961–970.
- Bressler SL. 1990. The gamma wave: a cortical information carrier? *Trends Neurosci* 13:161–162.
- Cobb SR, Buhl EH, Halasy K, Paulsen O, Somogyi P. 1995. Synchronization of neuronal activity in hippocampus by individual GABAergic interneurons. *Nature* 378:75–78.
- Colling SB, Stanford IM, Traub RD, Jefferys JG. 1998. Limbic gamma rhythms. I. Phase-locked oscillations in hippocampal CA1 and subiculum. *J Neurophysiol* 80:155–161.
- Colom LV, Nassif-Caudarella S, Dickson CT, Smythe JW, Bland BH. 1991. *In vivo* intrahippocampal microinfusion of carbachol and bicuculline induces theta-like oscillations in the septally deafferented hippocampus. *Hippocampus* 1:381–390.
- Demiralp T, Basar-Eroglu C, Basar E. 1996. Distributed gamma band responses in the brain studied in cortex, reticular formation, hippocampus and cerebellum. *Int J Neurosci* 84:1–13.
- Dickson CT, Alonso A. 1997. Muscarinic induction of synchronous population activity in the entorhinal cortex. *J Neurosci* 17:6729–6744.
- Dutar P, Bassant MH, Senut MC, Lamour Y. 1995. The septohippocampal pathway: structure and function of a central cholinergic system. *Physiol Rev* 75:393–427.
- Fellous JM, Sejnowski TJ. 1998. The involvement of CA1 and CA3 in carbachol-induced oscillations in the hippocampal slice. *Soc Neurosci Abstr* 24:1582.
- Fellous JM, Johnston T, Segal M, Lisman JE. 1998. Carbachol-Induced rhythms in the hippocampal slice: slow (.5–2Hz), theta (4–10Hz) and gamma (80–100Hz) oscillations. In: Bower JM, editor. *Computational neuroscience: trends in research*. New York: Plenum Press. p 367–372.
- Fisahn A, Pike FG, Buhl EH, Paulsen O. 1998. Cholinergic induction of network oscillations at 40 Hz in the hippocampus *in vitro* [see comments]. *Nature* 394:186–189.
- Fischer Y, Gähwiler BH, Thompson SM. 1999. Activation of intrinsic hippocampal theta oscillations by acetylcholine in rat septo-hippocampal cocultures. *J Physiol (Lond)* 519:405–413.
- Freund TF, Antal M. 1988. GABA-containing neurons in the septum control inhibitory interneurons in the hippocampus. *Nature* 336:170–173.
- Frotscher M, Leranth C. 1985. Cholinergic innervation of the rat hippocampus as revealed by choline acetyltransferase immunocytochemistry: a combined light and electron microscopic study. *J Comp Neurol* 239:237–246.
- Gray CM. 1994. Synchronous oscillations in neuronal systems: mechanisms and functions. *J Comput Neurosci* 1:11–38.
- Grunze HC, Rainnie DG, Hasselmo ME, Barkai E, Hearn EF, McCarley RW, Greene RW. 1996. NMDA-dependent modulation of CA1 local circuit inhibition. *J Neurosci* 16:2034–2043.
- Heynen AJ, Bilkey DK. 1991. Induction of RSA-like oscillations in both the *in-vitro* and *in-vivo* hippocampus. *Neuroreport* 2:401–404.
- King C, Recce M, O’Keefe J. 1998. The rhythmicity of cells of the medial septum/diagonal band of Broca in the awake freely moving rat: relationships with behaviour and hippocampal theta. *Eur J Neurosci* 10:464–477.
- Kirk IJ, McNaughton N. 1993. Mapping the differential effects of procaine on frequency and amplitude of reticularly elicited hippocampal rhythmic slow activity. *Hippocampus* 3:517–525.
- Konopacki J. 1998. Theta-like activity in the limbic cortex *in vitro*. *Neurosci Biobehav Rev* 22:311–323.
- Konopacki J, Golebiewski H. 1993. Theta-like activity in hippocampal formation slices: cholinergic- GABAergic interaction. *Neuroreport* 4:963–966.
- Konopacki J, MacIver MB, Bland BH, Roth SH. 1987. Carbachol-induced EEG “theta” activity in hippocampal brain slices. *Brain Res* 405:196–198.
- Lee MG, Chrobak JJ, Sik A, Wiley RG, Buzsaki G. 1994. Hippocampal theta activity following selective lesion of the septal cholinergic system. *Neuroscience* 62:1033–1047.
- Leung LS, Yim CY. 1993. Rhythmic delta-frequency activities in the nucleus accumbens of anesthetized and freely moving rats. *Can J Physiol Pharmacol* 71:311–320.
- Leung LS, Yu HW. 1998. Theta-frequency resonance in hippocampal CA1 neurons *in vitro* demonstrated by sinusoidal current injection. *J Neurophysiol* 79:1592–1596.
- Leung LW, Desborough KA. 1988. APV, an N-methyl-D-aspartate receptor antagonist, blocks the hippocampal theta rhythm in behaving rats. *Brain Res* 463:148–152.
- Leung LW, Yim CY. 1991. Intrinsic membrane potential oscillations in hippocampal neurons *in vitro*. *Brain Res* 553:261–274.

- Leung LW, Lopes da Silva FH, Wadman WJ. 1982. Spectral characteristics of the hippocampal EEG in the freely moving rat. *Electroencephalogr Clin Neurophysiol* 54:203–219.
- Liljenstrom H, Hasselmo ME. 1995. Cholinergic modulation of cortical oscillatory dynamics. *J Neurophysiol* 74:288–297.
- Lytton WW, Sejnowski TJ. 1991. Simulations of cortical pyramidal neurons synchronized by inhibitory interneurons. *J Neurophysiol* 66:1059–1079.
- MacVicar BA, Tse FW. 1989. Local neuronal circuitry underlying cholinergic rhythmical slow activity in CA3 area of rat hippocampal slices. *J Physiol (Lond)* 417:197–212.
- Madison DV, Lancaster B, Nicoll RA. 1987. Voltage clamp analysis of cholinergic action in the hippocampus. *J Neurosci* 7:733–741.
- McCormick DA. 1989. Cholinergic and noradrenergic modulation of thalamocortical processing [see comments]. *Trends Neurosci* 12:215–221.
- McMahon LL, Williams JH, Kauer JA. 1998. Functionally distinct groups of interneurons identified during rhythmic carbachol oscillations in hippocampus in vitro. *J Neurosci* 18:5640–5651.
- Meador KJ, Thompson JL, Loring DW, Murro AM, King DW, Gallagher BB, Lee GP, Smith JR, Flanigin HF. 1991. Behavioral state-specific changes in human hippocampal theta activity. *Neurology* 41:869–872.
- Monmaur P, Ayadi K, Breton P. 1993. Hippocampal EEG responses induced by carbachol and atropine infusions into the septum and the hippocampus in the urethane-anesthetized rat. *Brain Res* 631:317–324.
- Monmaur P, Collet A, Puma C, Frankel-Kohn L, Sharif A. 1997. Relations between acetylcholine release and electrophysiological characteristics of theta rhythm: a microdialysis study in the urethane-anesthetized rat hippocampus. *Brain Res Bull* 42:141–146.
- Oddie SD, Bland BH, Colom LV, Vertes RP. 1994. The midline posterior hypothalamic region comprises a critical part of the ascending brainstem hippocampal synchronizing pathway. *Hippocampus* 4:454–473.
- Patil MM, Hasselmo ME. 1999. Modulation of inhibitory synaptic potentials in the piriform cortex. *J Neurophysiol* 81:2103–2118.
- Penttonen M, Kamondi A, Acsady L, Buzsaki G. 1998. Gamma frequency oscillation in the hippocampus of the rat: intracellular analysis in vivo. *Eur J Neurosci* 10:718–728.
- Pitler TA, Alger BE. 1992. Cholinergic excitation of GABAergic interneurons in the rat hippocampal slice. *J Physiol (Lond)* 450:127–142.
- Riekkinen P, Buzsaki G, Riekkinen P Jr, Soinen H, Partanen J. 1991. The cholinergic system and EEG slow waves. *Electroencephalogr Clin Neurophysiol* 78:89–96.
- Smythe JW, Christie BR, Colom LV, Lawson VH, Bland BH. 1991. Hippocampal theta field activity and theta-on/theta-off cell discharges are controlled by an ascending hypothalamo-septal pathway. *J Neurosci* 11:2241–2248.
- Soltész I, Deschenes M. 1993. Low- and high-frequency membrane potential oscillations during theta activity in CA1 and CA3 pyramidal neurons of the rat hippocampus under ketamine-xylazine anesthesia. *J Neurophysiol* 70:97–116.
- Steriade M, Amzica F, Nunez A. 1993a. Cholinergic and noradrenergic modulation of the slow (approximately 0.3 Hz) oscillation in neocortical cells. *J Neurophysiol* 70:1385–400.
- Steriade M, Contreras D, Curro Dossi R, Nunez A. 1993b. The slow (1 Hz) oscillation in reticular thalamic and thalamocortical neurons: scenario of sleep rhythm generation in interacting thalamic and neocortical networks. *J Neurosci* 13:3284–3299.
- Steriade M, McCormick DA, Sejnowski TJ. 1993c. Thalamocortical oscillations in the sleeping and aroused brain. *Science* 262:679–685.
- Steriade M, Nunez A, Amzica F. 1993d. Intracellular analysis of relations between the slow (<1 Hz) neocortical oscillation and other sleep rhythms of the electroencephalogram. *J Neurosci* 13:3266–3283.
- Steriade M, Nunez A, Amzica F. 1993e. A novel slow (<1 Hz) oscillation of neocortical neurons in vivo: depolarizing and hyperpolarizing components. *J Neurosci* 13:3252–3265.
- Stewart M, Fox SE. 1990. Do septal neurons pace the hippocampal theta rhythm? *Trends Neurosci* 13:163–168.
- Timofeev I, Steriade M. 1996. Low-frequency rhythms in the thalamus of intact-cortex and decorticated cats. *J Neurophysiol* 76:4152–4168.
- Toth K, Freund TF, Miles R. 1997. Disinhibition of rat hippocampal pyramidal cells by GABAergic afferents from the septum. *J Physiol (Lond)* 500:463–474.
- Traub RD, Miles R, Buzsaki G. 1992. Computer simulation of carbachol-driven rhythmic population oscillations in the CA3 region of the in vitro rat hippocampus. *J Physiol (Lond)* 451:653–672.
- Traub RD, Whittington MA, Colling SB, Buzsaki G, Jefferys JG. 1996. Analysis of gamma rhythms in the rat hippocampus in vitro and in vivo. *J Physiol (Lond)* 493:471–484.
- Vertes RP. 1982. Brain stem generation of the hippocampal EEG. *Prog Neurobiol* 19:159–186.
- Vinogradova OS. 1995. Expression, control and probable functional significance of the neuronal theta-rhythm. *Prog Neurobiol* 45:523–583.
- Wang XJ, Buzsaki G. 1996. Gamma oscillation by synaptic inhibition in a hippocampal interneuronal network model. *J Neurosci* 16:6402–6413.
- Whittington MA, Traub RD, Jefferys JG. 1995. Synchronized oscillations in interneuron networks driven by metabotropic glutamate receptor activation [see comments]. *Nature* 373:612–615.
- Wiig KA, Heynen AJ, Bilkey DK. 1994. Effects of kainic acid microinfusions on hippocampal type 2 RSA (theta). *Brain Res Bull* 33:727–732.
- Williams JH, Kauer JA. 1997. Properties of carbachol-induced oscillatory activity in rat hippocampus. *J Neurophysiol* 78:2631–2640.
- Ylinen A, Bragin A, Nadasdy Z, Jando G, Szabo I, Sik A, Buzsaki G. 1995a. Sharp wave-associated high-frequency oscillation (200 Hz) in the intact hippocampus: network and intracellular mechanisms. *J Neurosci* 15:30–46.
- Ylinen A, Soltész I, Bragin A, Penttonen M, Sik A, Buzsaki G. 1995b. Intracellular correlates of hippocampal theta rhythm in identified pyramidal cells, granule cells, and basket cells. *Hippocampus* 5:78–90.
- Zhang S, Jose JV, Tiesinga PHE. 2000. Model of carbachol-induced gamma-frequency oscillations in hippocampus. *CNS 1999, Pittsburgh. Neurocomputing* (in press).
- Zhang Y, Perez Velazquez JL, Tian GF, Wu C, Skinner FK, Carlen PL, Zhang L. 1998. Slow oscillations (≈ 1 Hz) mediated by GABAergic interneuronal networks in rat hippocampus. *J Neurosci* 18:9256–9268.